

# Robust Discrete Time Tracking Control Using Sliding Surfaces

Seung Ho Cho\*

(Received May 30, 1994)

This paper deals with the robustness issues associated with the feedforward tracking control with respect to unmodeled plant uncertainties. Based on the Diophantine equation, a new discrete time sliding functions has been defined and utilized for the robust feedforward tracking control law. The robustness is achieved by using a sliding function-based nonlinear feedback. As for model/plant mismatches the plant order uncertainty and parameter uncertainty are taken into account for robustness analysis. Noncircular machining has been adopted as an application example of this algorithm. Through computer simulation it has been shown that the robust discrete time tracking control is effective for unmodeled plant uncertainties.

**Key Words:** Robustness, Unmodeled Plant Uncertainty, Sliding Function, Feedforward Tracking Control, Noncircular Machining

## 1. Introduction

In servoproblems, the feedback controller is not sufficient for assuring good tracking performance when the desired position is time varying. The tracking performance can be significantly improved by the feedforward controller, the design of which is based on the inversion of a dynamical model which describes the controlled plant and feedback controller. It is used as a prefilter for processing the desired output so that the overall transfer function from the desired output to the actual output becomes close to unity. In designing feedforward tracking controllers, different approaches may be taken depending on whether the plant is a minimum phase system or a non-minimum phase system. This paper is concerned with minimum phase system. For minimum phase systems the feedforward tracking controller can be designed to achieve perfect tracking based on stable pole/zero cancellation. Given the desired trajectory, the optimal linear tracking approach (Anderson and Moore, 1971), previous control approach (Tomizuka and Whitney, 1975),

and independent tracking and regulation approach (Landau and Lozano, 1981) are well known to be effective for the purpose of tracking.

The control schemes discussed above are based on the assumption that the plant is accurately known. In fact the model/plant mismatches may significantly degrade tracking performance and even result in the instabilities of the overall system. These model/plant mismatches are due to modeling errors, which consist of parameter (structural) uncertainty and order (unstructural) uncertainty, and disturbances etc.. In this paper a discrete time version of variable structure control (Utkin, 1977) is applied to enhance the robustness of perfect tracking control. We construct the nonlinear feedback control law which is based on discrete time sliding function. This paper extends the idea of (Kreisselmeier and Anderson, 1986) to the proof of boundedness of control input and of output signal. As an application example of this algorithm, noncircular machining (Higuchi et al, 1984) is adopted for computer simulation.

The remainder of this paper is organized as follows. Section 2 describes the formulation of the problem. Section 3 describes the robust discrete time tracking control algorithm and analyzes the

\* Department of Mechanical Engineering Hong-Ik University Mapo-Ku, Seoul 121-791, Korea

stability of robust discrete time tracking control system. Section 4 describes the numerical example of noncircular machining. Conclusions are given in Sec. 5.

## 2. Formulation of the Problem

The controlled plant is assumed to be represented by the following discrete time model :

$$y(k) = \frac{z^{-d}B(z^{-1})}{A(z^{-1})} u(k) + \eta(k) \quad (1)$$

where

- $u(k)$  and  $y(k)$  are the measurable input and output respectively,
- $\eta(k)$  represents the modeling error,
- $A(z^{-1})$  and  $B(z^{-1})$  are polynomials in the backward shift operator  $z^{-1}$ , of the form  
 $A(z^{-1}) = 1 + a_1z^{-1} + \dots + a_nz^{-n}$ ,  
 $B(z^{-1}) = b_0 + b_1z^{-1} + \dots + b_mz^{-m}$ ,  $b_0 \neq 0$ .

The order  $n$  and  $m$  as well as the delay step  $d$  are assumed to be known. It is further assumed that (Kreisselmeier and Anderson, 1986)

- A1 :  $A(z^{-1})$  and  $B(z^{-1})$  are coprime.  
A2 :  $|\eta(k)| \leq \mu m(k)$ , where  $\mu$  is a positive scalar and  $m(k)$  is defined by

$$m(k) = \sigma m(k-1) + |u(k-1)| + |y(k-1)|, \quad 0 < \sigma < 1. \quad (2)$$

- A3 :  $\|\theta_i\| \leq \rho_1$ , where  $\theta_i^T = [a_1, \dots, a_n, b_0, \dots, b_m]$  and  $\rho_1$  is a known positive scalar.

The plant(1) can also be expressed as

$$y(k) = \theta_1^T \phi_1(k) + \eta_1(k) \quad (3)$$

where

$$\phi_1^T(k) = \{-y(k-1), \dots, -y(k-n), u(k-d), \dots, u(k-d-m)\}, \\ \eta_1(k) = A(z^{-1})\eta(k).$$

Then it follows from A2-A3 and (2) that

$$|\eta_1(k)| = |A(z^{-1})\eta(k)| \leq \nu_1 \mu m(k) \quad (4)$$

with

$$\nu_1 = 1 + \rho_1 \sigma^{-n} \quad (5)$$

which is derived in Appendix.

## 3. Robust Discrete Time Tracking Control

We achieve perfect tracking control by stable pole/zero cancellation. In this paper we propose a robust discrete time tracking control by combining pole/zero cancellation and discrete time version of sliding control. For assignment of closed loop poles and setting the structure of the control system, we utilize the following Diophantine equation.

$$D_1(z^{-1}) = A(z^{-1})S_1(z^{-1}) + z^{-d}R_1(z^{-1}) \quad (6)$$

where

$$R_1(z^{-1}) = r_0 + r_1z^{-1} + \dots + r_{n-1}z^{-(n-1)}, \\ S_1(z^{-1}) = 1 + s_1z^{-1} + \dots + s_{d-1}z^{-(d-1)}, \\ D_1(z^{-1}) = 1 + d_1z^{-1} + \dots + d_nz^{-n}.$$

From Eqs. (6) and (1), the following equation is derived.

$$D_1(z^{-1})y(k) = \theta_2^T \phi_2(k-d) + \eta_2(k) \quad (7)$$

where

$$\theta_2^T = (b_0, b_0s_1 + b_1, \dots, b_ms_{d-1}, r_0, r_1, \dots, r_{n-1}), \quad (8)$$

$$\phi_2^T(k) = \{u(k), u(k-1), \dots, u(k-m-d+1), y(k), y(k-1), \dots, y(k-n+1)\}. \quad (9)$$

and  $\eta_2(k)$  is expressed as follows

$$\eta_2(k) = \theta_7^T \phi_7(k) \quad (11)$$

where

$$\theta_7^T = (1, a_1 + s_1, \dots, a_ns_{d-1}), \\ \phi_7^T(k) = \{\eta(k), \eta(k-1), \dots, \eta(k-n-d+1)\}.$$

To derive the bounds of  $|\theta_2^T \phi_2(k-d)|$  and  $|\eta_2(k)|$  it is necessary to have the following assumption.

- A4 :  $\|\theta_d\| \leq \rho_2$ , where  $\theta_d^T = (s_1, s_2, \dots, s_{d-1}, r_0, r_1, \dots, r_{n-1})$  and  $\rho_2$  is a known positive scalar.

**Proposition 1**  $|\theta_2^T \phi_2(k-d)| \leq K_{m1} \sigma^{1-d-r} m(k)$ ,

where  $r = \max \deg(n, m+d)$ ,

$$K_{m1} = (m+1)\rho_1 + (m+1)(d-1)\rho_1\rho_2 + n\rho_2.$$

Proof :

$$|\theta_2^T \phi_2(k-d)|$$

$$\begin{aligned}
&= |S_1(z^{-1})B(z^{-1})u(k-d) \\
&\quad + R_1(z^{-1})y(k-d)| \\
&= \left| \left( 1 + \sum_{i=1}^{d-1} s_i z^{-i} \right) \sum_{i=0}^m b_i z^{-r} u(k-d) \right. \\
&\quad \left. + \sum_{i=0}^{n-1} r_i z^{-i} y(k-d) \right| \\
&\leq \left| \sum_{i=0}^m b_i u(k-d-i) \right| + \left| \sum_{i=0}^{n-1} r_i y(k-d-i) \right| \\
&\quad + \left| \sum_{i=1}^{d-1} s_i z^{-i} \sum_{i=0}^m b_i z^{-i} u(k-d) \right|. \quad (12)
\end{aligned}$$

The first term of (12) becomes

$$\begin{aligned}
&\left| \sum_{i=0}^m b_i u(k-d-i) \right| \\
&\leq |b_0 u(k-d)| + |b_1 u(k-d-1)| \\
&\quad + \cdots + |b_m u(k-d-m)| \\
&\leq |b_0| \sigma^{1-d} m(k) + |b_1| \sigma^{1-d-1} m(k) \\
&\quad + \cdots + |b_m| \sigma^{1-d-m} m(k) \\
&\leq (|b_0| + |b_1| + \cdots + |b_m|) \sigma^{1-d-m} m(k) \\
&\leq (m+1) \rho_1 \sigma^{1-d-m} m(k). \quad (13)
\end{aligned}$$

Similarly the second term of (12) becomes

$$\left| \sum_{i=0}^{n-1} r_i y(k-d-i) \right| \leq n \rho_2 \sigma^{1-d-n+1} m(k). \quad (14)$$

The third term of (12) becomes

$$\begin{aligned}
&\left| \sum_{i=1}^{d-1} s_i z^{-i} \sum_{i=0}^m b_i z^{-i} u(k-d) \right| \\
&= \left| (s_1 z^{-1} + s_2 z^{-2} + \cdots + s_{d-1} z^{-(d-1)}) \right. \\
&\quad \left. \sum_{i=0}^m b_i z^{-i} u(k-d) \right| \\
&\leq |s_1| \sum_{i=0}^m b_i z^{-i-1} u(k-d) + |s_2| \sum_{i=0}^m b_i z^{-i-2} u(k-d) \\
&\quad + \cdots + |s_{d-1}| \sum_{i=0}^m b_i z^{-i-(d-1)} u(k-d). \quad (15)
\end{aligned}$$

Each term of (15) can be expressed as follows.

$$\begin{aligned}
&\left| s_1 \sum_{i=0}^m b_i z^{-i-1} u(k-d) \right| \\
&= \left| s_1 \sum_{i=0}^m b_i u(k-d-i-1) \right| \\
&\leq |s_1| \sum_{i=0}^m |b_i| |u(k-d-i-1)| \\
&\leq |s_1| \rho_1 (m+1) \sigma^{1-d-m-1} m(k) \quad (16)
\end{aligned}$$

$$\begin{aligned}
&\left| s_2 \sum_{i=0}^m b_i z^{-i-2} u(k-d) \right| \\
&= \left| s_2 \sum_{i=0}^m b_i u(k-d-i-2) \right| \\
&\leq |s_2| \sum_{i=0}^m |b_i| |u(k-d-i-2)| \\
&\leq |s_2| \rho_1 (m+1) \sigma^{1-d-m-2} m(k) \quad (17) \\
&\vdots
\end{aligned}$$

$$\begin{aligned}
&\left| s_{d-1} \sum_{i=0}^m b_i z^{-i-(d-1)} u(k-d) \right| \\
&= \left| s_{d-1} \sum_{i=0}^m b_i u\{k-d-i-(d-1)\} \right| \\
&\leq |s_{d-1}| \sum_{i=0}^m |b_i| |u\{k-d-i-(d-1)\}| \\
&\leq |s_{d-1}| \rho_1 (m+1) \sigma^{1-d-m-(d-1)} m(k). \quad (18)
\end{aligned}$$

Substituting (16), (17), and (18) into (15) leads to

$$\begin{aligned}
&\left| \sum_{i=1}^{d-1} s_i z^{-i} \sum_{i=0}^m b_i z^{-i} u(k-d) \right| \\
&\leq (|s_1| + |s_2| + \cdots + |s_{d-1}|) \\
&\quad \cdot \rho_1 (m+1) \sigma^{1-d-m-(d-1)} m(k) \\
&\leq \rho_1 (m+1) \rho_2 (d-1) \sigma^{1-d-m-(d-1)} m(k). \quad (19)
\end{aligned}$$

Finally substituting (13), (14) and (19) into (12) leads to

$$\begin{aligned}
&|\theta_2^T \phi_2(k-d)| \\
&\leq (m+1) \rho_1 \sigma^{1-d-m-(d-1)} m(k) \\
&\quad + \rho_1 \rho_2 (m+1) (d-1) \sigma^{1-d-m-(d-1)} m(k) \\
&\quad + n \rho_2 \sigma^{1-d-n+1} m(k) \\
&\leq K_{m1} \sigma^{1-d-r} m(k). \quad (20)
\end{aligned}$$

It follows with assumption A4 that

$$|\eta_2(k)| = |A(z^{-1})S_1(z^{-1})\eta(k)| \leq \nu_2 \mu m(k) \quad (21)$$

with

$$\nu_2 = 1 + 3 \rho_1 \rho_2 n (d-1) \sigma^{-n-(d-1)} \quad (22)$$

which is derived in Appendix.

For  $\eta_2(k)=0$ , the control law for regulation and tracking can be obtained by letting the tracking error satisfy

$$D_1(z^{-1})[y(k+d) - y_m(k+d)] = 0 \quad (23)$$

where  $y_m(k)$  is the desired output.

From Eqs. (6) and (23), the control law is

$$\begin{aligned}
u(k) &= \frac{1}{b_0} [D_1(z^{-1})y_m(k+d) - \bar{\theta}_2^T \bar{\phi}_2(k)] \\
&= \frac{A(z^{-1})}{D_1(z^{-1})B(z^{-1})} y^*(k+d) \quad (24)
\end{aligned}$$

where  $\bar{\theta}_2$  and  $\bar{\phi}_2(k)$  are defined by

$$\bar{\theta}_2^T = [b_0, \bar{\theta}_2^T] \quad (25)$$

$$\bar{\phi}_2^T(k) = [u(k), \bar{\phi}_2^T(k)] \quad (26)$$

and

$$y^*(k) = D_1(z^{-1})y_m(k).$$

For  $\eta_2(k) \neq 0$ , Eq. (23) is not achieved under the control law (24).

In designing a robust discrete time tracking

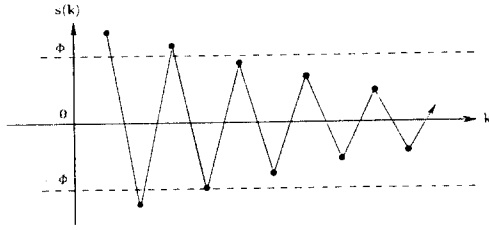


Fig. 1 Sliding surface with boundary layer

controller we define  $s(k)$  by

$$s(k) = D_1(z^{-1})[y(k) - y_m(k)] \quad (27)$$

and add a control loop with  $s(k)$  to compensate the modeling error  $\eta_2(k)$ . While it is not possible to let  $s(k) = 0$ , this additional control loop resembles the sliding mode control for continuous time systems. Outside the boundary layer ( $|s(k)| \geq \Phi$ ) as well as inside the boundary layer ( $|s(k)| < \Phi$ ) the control law (24) is now modified to

$$u(k) = \frac{1}{b_0} \left[ s(k) + D_1(z^{-1})y_m(k+d) - \bar{\theta}_2^T \bar{\phi}_2(k) - K \text{sat} \left\{ \frac{s(k)}{\Phi} \right\} \right]$$

$$= \frac{A(z^{-1})}{D_1(z^{-1})B(z^{-1})} \left[ s(k) + y^*(k+d) - K \text{sat} \left\{ \frac{s(k)}{\Phi} \right\} \right] \quad (28)$$

where

$$\text{sat} \left\{ \frac{s(k)}{\Phi} \right\} = \begin{cases} +1, & \text{for } \phi \leq s(k), \\ \frac{s(k)}{\Phi}, & \text{for } -\Phi < s(k) < \Phi, \\ -1, & \text{for } s(k) \leq -\Phi, \end{cases} \quad (29)$$

and  $\bar{\theta}_2$  and  $\bar{\phi}_2(k)$  are defined by (25) and (26).

$\Phi$  determines the size of the boundary layer around  $s(k) = 0$ .  $s(k)$  is expected to behave as illustrated in Fig. 1. The overall block diagram of the robust discrete time tracking control system becomes as shown in Fig. 2, where  $S_{B1}(z^{-1}) = B(z^{-1})S_1(z^{-1}) - b_0$ .

**Proposition 2)** For arbitrary  $d_0 > 0$  there exists a  $\mu_0 > 0$  (which depends on  $d_0$ ) such that for all  $0 \leq \mu \leq \mu_0$  and arbitrary initial conditions, it follows that

$$|S(k)| \leq d_0 m(K)$$

**Proof:** Since the reference input  $y_m(k)$  is bounded in modulus by a known constant and  $D_1(z^{-1})$  is a strictly stable polynomial,

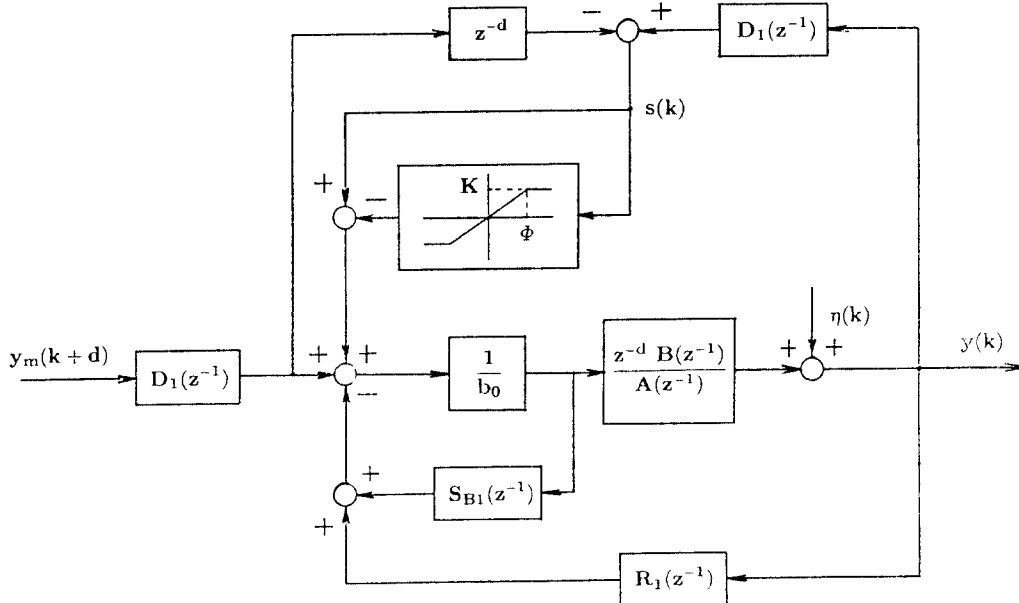


Fig. 2 Robust discrete time tracking control system

$$\begin{aligned}
|s(k)| &= |D_1(z^{-1})y(k) - D_1(z^{-1})y_m(k)| \\
&= |\eta_2(k)| \\
&\leq \nu_2 \mu m(k) \\
&\leq d_0 m(k)
\end{aligned} \tag{30}$$

where

$$d_0 = \nu_2 \mu_0.$$

**Proposition 3)**  $m(k)$  is bounded, in turn  $u(k)$  and  $y(k)$  are bounded.

Proof: Since  $D_1(z^{-1})$  is a strictly stable polynomial, let  $\frac{1}{D_1(z^{-1})}$  and  $\frac{A(z^{-1})}{D_1(z^{-1})B(z^{-1})}$  be both exponentially bounded in modulus by  $K_p$  and in exponent by  $\sigma_p$ . Then we get

$$\begin{aligned}
|y(k-1)| &\leq \frac{K_p}{1-\sigma_p z^{-1}} \\
\cdot \{ &|s(k-1)| + |y^*(k-1)| \}.
\end{aligned} \tag{31}$$

Outside the sliding boundary layer

$$\begin{aligned}
|u(k-1)| &\leq \frac{K_p}{1-\sigma_p z^{-1}} \\
\cdot \{ &|s(k-1)| + |y^*(k+d-1)| + K \}.
\end{aligned} \tag{32}$$

Further (2), (31) and (32) yield

$$\begin{aligned}
m(k) &\leq \sigma m(k-1) + \frac{K_p}{1-\sigma_p z^{-1}} \{ |s(k-1)| + |y^*(k-1)| \} \\
&\quad + \frac{K_p}{1-\sigma_p z^{-1}} \{ |s(k-1)| + |y^*(k+d-1)| + K \} \\
&\leq \sigma m(k-1) + \frac{K_p}{1-\sigma_p z^{-1}} \{ d_0 m(k-1) + |y^*(k-1)| \} \\
&\quad + \frac{K_p}{1-\sigma_p z^{-1}} \{ d_0 m(k-1) + |y^*(k+d-1)| + K \}
\end{aligned} \tag{33}$$

Defining

$$\begin{aligned}
r^*(k) &= \frac{K_p}{1-\sigma_p z^{-1}} \{ |y^*(k-1)| + |y^*(k+d-1)| + K \}.
\end{aligned} \tag{34}$$

it follows

$$\begin{aligned}
m(k) &\leq \sigma m(k-1) + \frac{2K_p d_0}{1-\sigma_p z^{-1}} m(k-1) + r^*(k).
\end{aligned} \tag{35}$$

Let  $\bar{m}(k)$  be an upper bound of  $m(k)$ , then (35) can be expressed as

$$\bar{m}(k) = \sigma \bar{m}(k-1) + \frac{2K_p d_0}{1-\sigma_p z^{-1}} \bar{m}(k-1)$$

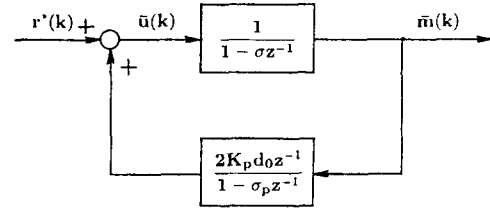


**Fig. 3** Feedback configuration for the robust stability investigation

$$+ r^*(k). \tag{36}$$

It can also be written as

$$(1-\sigma z^{-1})\bar{m}(k) = r^*(k) + \frac{2K_p d_0 z^{-1}}{1-\sigma_p z^{-1}} \bar{m}(k) \tag{37}$$

or, equivalently, as the feedback system

$$\bar{u}(k) = r^*(k) + \frac{2K_p d_0 z^{-1}}{1-\sigma_p z^{-1}} \bar{m}(k) \tag{38}$$

$$\bar{m}(k) = \frac{1}{1-\sigma z^{-1}} \bar{u}(k) \tag{39}$$

which is depicted in Fig. 3.

Its closed-loop characteristic equation is

$$C_l(z^{-1}) = (1-\sigma z^{-1})(1-\sigma_p z^{-1}) - 2K_p d_0 z^{-1} = 0. \tag{40}$$

Boundedness of  $\bar{m}(k)$  is guaranteed if  $C_l(1) > 0$ , i.e.,

$$(1-\sigma)(1-\sigma_p) - 2K_p d_0 > 0. \tag{41}$$

Since  $\bar{m}(k)$  is an upperbound of  $m(k)$ , the boundedness of  $\bar{m}(k)$  in turn assures the boundedness of all signals of the robust discrete time tracking control system. Noting that  $\sigma, \sigma_p$  lie in  $(0,1)$  it is not hard to see that the stability of the feedback configuration (38), (39) is obtained if  $d_0$  is chosen so that  $d_0 > 0$  and

$$2K_p d_0 < (1-\sigma)(1-\sigma_p). \tag{42}$$

The condition that  $\Phi$  and  $K$  satisfy will be explained in theorem.

Notice that from Eqs. (27) and (28),  $s(k)$  satisfies

$$s(k+d) = s(k) + \eta_2(k+d) - K \text{sat} \left\{ \frac{s(k)}{\Phi} \right\}. \tag{43}$$

The robust stability of the robust discrete time tracking control system is proved in the following theorem.

**Theorem : Robust Stability of the Robust Dis-**

crete Time Tracking Control System :

The robust discrete time tracking control system, consisting of the plant(1) and the control law(28), is stable in the sense that  $|s(k)|$  decreases when  $|s(k)| > \Phi$  and that the steady state value of  $s$  is bounded by  $\Phi$ .

Proof: Introduce the following discrete Lyapunov function candidate

$$V(k) = |s(k)| \quad (44)$$

which can be interpreted as the distance to the surface  $s(k) = 0$ .

Then we can formulate the following difference equation.

$$\begin{aligned} \Delta V_i(k+d) &= V_i(k+d) - V_i(k), \quad i=1, 2, \dots, d, \\ &= |s_i(k+d)| - |s_i(k)| \\ &= |s_i(k) + \eta_2(k+d) - K \operatorname{sgn}\{s_i(k)\}| \\ &\quad - |s_i(k)| \end{aligned} \quad (45)$$

where the sliding function and Lyapunov function with subscript  $i$  are defined as follows.

- $s_1(k)$ ,  $V_1(k)$  :  $k$  takes values  $0, d, 2d, 3d, \dots$
- $s_2(k)$ ,  $V_2(k)$  :  $k$  takes values  $1, d+1, 2d+1, 3d+1, \dots$
- $s_d(k)$ ,  $V_d(k)$  :  $k$  takes values  $d-1, 2d-1, 3d-1, 4d-1, \dots$

Based on the Proposition 3 let us assume that the upperbound of modeling error is constant, i.e.

$$|\eta_2(k)| \leq \nu_2 \mu m(k) \leq F_2 \quad (46)$$

where  $F_2$  is a bounded scalar. Then the following two conditions on  $K$  make (45) negative.

$$K > F_2, \quad K > 2|s_i(k)| - F_2. \quad (47)$$

In designing a robust discrete time sliding controller it is desirable to reach the sliding surface as soon as possible at transient stage, which motivates the use of upperbound of modeling error.

The second condition on  $K$  is derived from the fact that between sampling instants the system behaves in open loop manner, which forces the distance from sliding boundary layer be decreased from stability viewpoint as the discrete-time  $k$  increases. So the minimum value of  $2|s_i(k)| - F_2$  is  $2\Phi - F_2$ .

If  $K$  is selected as following

$$K = F_2 + \eta_0 \quad (48)$$

where  $\eta_0$  is related to  $s(k+d) = s(k) - \eta_0 \operatorname{sgn}\{s(k)\}$ . If we want to use the discrete-time sliding controller for robustness even when there exists no modeling error in plant equation(1), i.e.,  $\eta(k) = 0$ , in light of the inherent property of sliding mode control we have to assume the boundary layer thickness, which is related to  $\eta_0$  in(48).

Then (44) will be a Lyapunov function in the following region.

$$|s_i(k)| > F_2 + \frac{\eta_0}{2}. \quad (49)$$

Inside the boundary layer, the  $s$ -dynamics become :

$$s(k+d) = \left(1 - \frac{K}{\Phi}\right)s(k) + \eta_2(k+d). \quad (50)$$

The boundary layer thickness  $\Phi$  can be selected such that (43) shows characteristics of a first-order filter with input  $\eta_2(k+d)$  and eigenvalue.

$$1 - \frac{K}{\Phi} = \lambda. \quad (51)$$

From (48) and (51) :

$$\Phi = \frac{F_2 + \eta_0}{1 - \lambda}. \quad (52)$$

From the stability viewpoint the following relation should be satisfied.

$$\left|1 - \frac{K}{\Phi}\right| < 1. \quad (53)$$

Then the solution takes the following forms :

$$\begin{aligned} s_1(k) &= \lambda^{\operatorname{int}(\frac{k}{d})} s(0) + \sum_{j=0}^{\operatorname{int}(\frac{k}{d})-1} \lambda^j \eta_2(k-j \cdot d) \\ s_2(k) &= \lambda^{\operatorname{int}(\frac{k}{d})} s(1) + \sum_{j=0}^{\operatorname{int}(\frac{k}{d})-1} \lambda^j \eta_2(k-j \cdot d) \\ &\vdots \\ s_d(k) &= \lambda^{\operatorname{int}(\frac{k}{d})} s(d-1) \\ &\quad + \sum_{j=0}^{\operatorname{int}(\frac{k}{d})-1} \lambda^j \eta_2(k-j \cdot d) \end{aligned} \quad (54)$$

Here "int" means integer value. In each equation of (54) the first term of right hand side represents transient solution, whereas the second term represents steady state solution. Although  $\eta_2(\cdot)$  is not fixed, it is a forcing term which is bounded and dominates steady state behavior.

For a stable eigenvalue  $\lambda$  the steady state solution becomes :

$$\lim_{k \rightarrow \infty} s_i(k) = \lim_{k \rightarrow \infty} \sum_{j=0}^{\infty} \lambda^j \eta_2(k-j \cdot d). \quad (55)$$

From (55) the following relations are derived.

$$|\lim_{k \rightarrow \infty} s(k)| \leq \{1 + |\lambda| + |\lambda|^2 + \dots\} F_2 \quad (56)$$

$$|\lim_{k \rightarrow \infty} s(k)| \leq \frac{1}{1-|\lambda|} F_2 < \frac{K}{1-|\lambda|} \quad (57)$$

$$|\lim_{k \rightarrow \infty} s(k)| < \Phi \quad (58)$$

#### 4. Numerical Example of Noncircular Machining

As an example of motion control the noncircular machining has been adopted with electrohydraulic servosystem for tool positioning. Noncircular machining is a turning operation which generates a workpiece with noncircular shaped cross-sections(Higuchi et al., 1984 and Tomizuka et al., 1987). Figure 4 shows the specification of noncircular cross-sectional shape of workpiece by a series of points, where the position of tool is controlled by hydraulic cylinder. The sampling period is determined by

$$T_s = \frac{1}{\left(\frac{n_s}{60}\right)N} \text{sec} \quad (59)$$

where  $n_s$  and  $N$  are the spindle speed in rpm and a required number of points to describe the cross-sectional shape, respectively. In this paper  $N=$

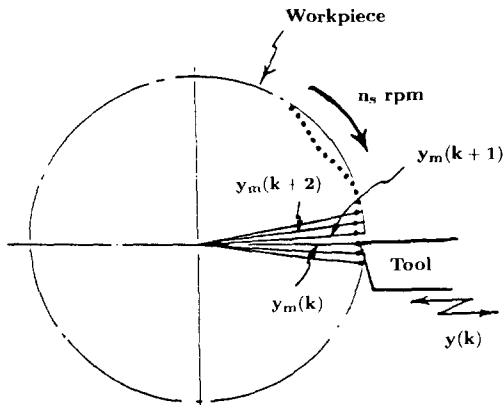


Fig. 4 Specification of noncircular cross-sectional shape

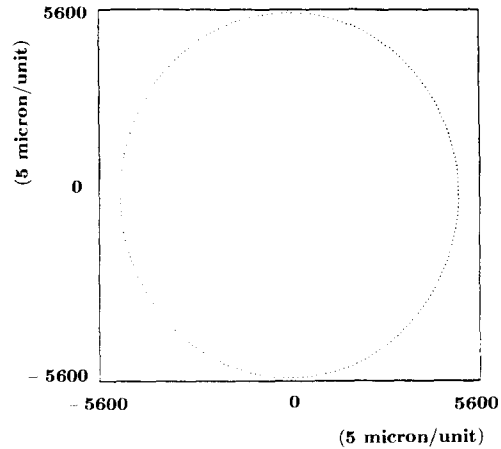


Fig. 5 Desired noncircular shape

250 and a nominal spindle speed of 600 rpm results in a sampling time of 0.4 msec.

Figure 5 shows the desired noncircular elliptical shape, which is obtained by letting the tool follow the signal in Fig. 6. The signal is repetitive with a period of 250 samples which are evenly spaced over one spindle revolution. Electrohydraulic servosystem is inherently nonlinear, but in this paper it has been idealized as a second order linear system(Higuchi et al, 1984).

Equations (60) and (61) describe the transfer function of electro-hydraulic servosystem in Laplace domain and z-domain respectively. The closed loop zero is expressed in Eq. (62), which is to be utilized for the design of robust discrete time tracking controller.

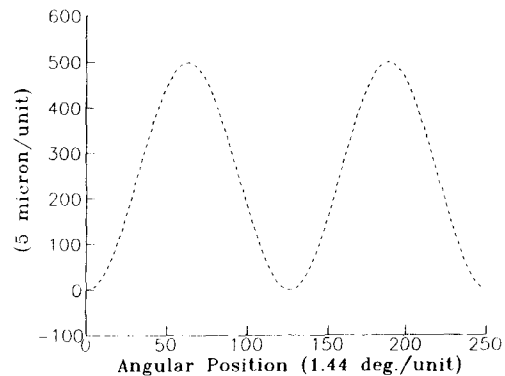


Fig. 6 Extended desired trajectory

$$\frac{Y(s)}{U(s)} = \frac{K_1}{s(1+T_1s)} \quad (60)$$

$$\frac{y(k)}{u(k)} = \frac{z^{-1}(b_0 + b_1z^{-1})}{1 + a_1z^{-1} + a_2z^{-2}} \quad (61)$$

$$\text{closed loop zero} = 1 + \frac{(T_s/T_1)(1 - e^{-T_s/T_1})}{1 - e^{-T_s/T_1} - T_s/T_1} \quad (62)$$

The following parametric values are used for the design of robust feedforward tracking controller.

$$(K_1, T_1) = (160, 0.002)$$

$$(a_1, a_2, b_0, b_1)$$

$$= (-1.81873, 0.81873, 0.00599, 0.00554)$$

$$\text{closed loop zero} = 0.9325 + 0j$$

The design parameters for controller are as follows.

$$\text{Diophantine Equation: } (0 - 0.2z^{-1})^2$$

$$\phi = 5.0, K = 0.5, \lambda = 0.9$$

The robust feedforward tracking controller as well as feedback controller has been designed based on the transfer function (60). Especially the closed loop zero becomes the pole of feedforward tracking controller. Once the closed loop zero is utilized for the design of feedforward tracking controller, the role of it ends up. Next our concern moves into the uncertainties of plant in order to show the effectiveness of robust discrete time tracking controller.

To consider the influence of the parameter and order uncertainty upon tracking performance, a couple of perturbed transfer functions have been utilized for simulation.

$$\frac{Y(s)}{U(s)} = \frac{K_2}{s(1+T_2s)} \quad (63)$$

$$\frac{Y(s)}{U(s)} = \frac{K_1}{s(1+T_1s)(1+T_3s)} \quad (64)$$

where,  $K_2 = 150$ ,  $T_2 = 0.005$ ,  $T_3 = 0.003$

Considering (61), the discrete time representation of (63) becomes :

$$\frac{y(k)}{u(k)} = \frac{z^{-1}[(b_0 + \delta b_0) + (b_1 + \delta b_1)z^{-1}]}{1 + (a_1 + \delta a_1)z^{-1} + (a_2 + \delta a_2)z^{-2}} \quad (65)$$

Equation (65) can be reconstructed to the form (66), which satisfies the assumption A2 in Sec. 2. In the similar way (64) can be discretized to the form satisfying the assumption A2.

$$y(k) = \frac{z^{-1}(b_0 + b_1z^{-1})}{1 + a_1z^{-1} + a_2z^{-2}} u(k)$$

$$- \frac{(\delta a_1 + \delta a_2 z^{-1})}{1 + a_1 z^{-1} + a_2 z^{-2}} y(k-1) + \frac{(\delta b_0 + \delta b_1 z^{-1})}{1 + a_1 z^{-1} + a_2 z^{-2}} u(k-1). \quad (66)$$

To conform the results thus obtained in Sec. 3. We are going to demonstrate whether the robust discrete time tracking control is really robust or not against the order uncertainty and parameter uncertainty when the closed loop zeros are located inside the unit circle. In simulation the numerical values of boundary layer thickness  $\phi$  and controller gain  $K$  are 5.0 and 0.5 respectively except the special cases for examining the effect of boundary layer thickness.

Figure 7 shows the control input and output error under the order uncertainty. Note in the figure that the robust discrete time tracking control is superior to perfect tracking control (PTC) when there is a model/plant mismatch in system order.

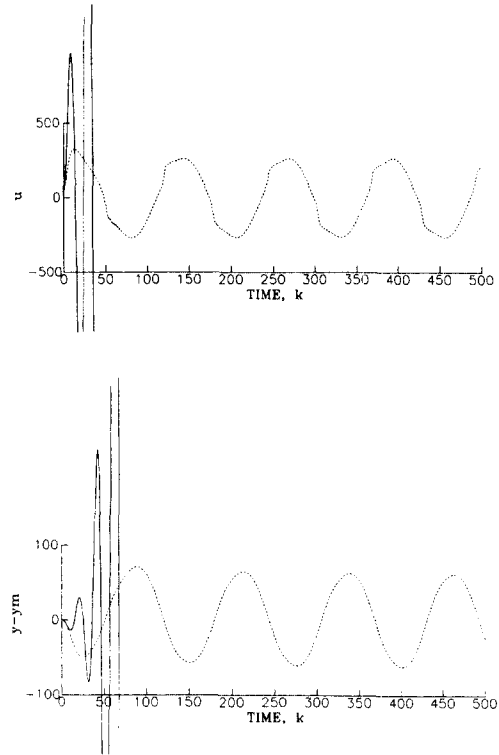
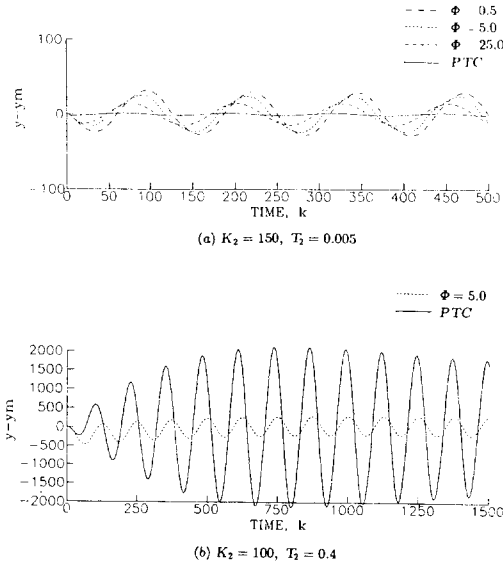


Fig. 7 Control input and output error under order uncertainty (solid : PTC, dot : robust discrete time tracking control)





**Fig. 8** Output error according to the boundary layer under parameter uncertainty

Figure 8 shows the output errors according to the boundary layer under parameter uncertainty. Both in Figs. 7 and 8 the discrete time scale of x-axis is 0.4 msec per unit. The scale of output error is 5 micron per unit.

We can observe in Fig. 8(a) that the robust discrete time tracking control is not superior to PTC in view of steady state error when the degree of parameter uncertainty is small. That characteristics are inevitable due to the inherent property of sliding control with saturation, which is supposed to admit a some degree of error for robustness. By manipulating the boundary layer  $\Phi$  the steady state performance can be increased to a satisfactory level, which is to be based on the degree of admissible output error. From these observations we need to trade off between the steady state performance and robustness under parameter uncertainty. When the degree of parameter uncertainty is large, the robust discrete time tracking control is superior to PTC as is shown in Fig. 8(b).

## 5. Conclusion

To increase the robustness of the feedforward tracking control system, a new discrete-time slid-

ing function has been defined based on Diophantine equation and utilized for the formulation of control law. The equation expressing the sliding boundary layer is composed of eigenvalue in s-dynamics and of upperbound in modeling error. The modeling error which ultimately affects on the tracking performance is diluted in the sliding boundary layer by way of saturation function, which results in increase of robustness. The performance of robust discrete time tracking controller can be examined in a couple of viewpoint, i.e., order uncertainty and parameter uncertainty. The robust discrete time tracking controller can be utilized more effectively than perfect tracking controller under plant order uncertainty when the closed loop zero is located on negative real axis inside the unit circle. But under parameter uncertainty a couple of contradictory phenomena have been observed due to the inherent property of sliding boundary layer. When the degree of parameter uncertainty is small, the output error under robust discrete time tracking control is larger than that under perfect tracking control. But as the degree of parameter uncertainty becomes large, the output error under robust discrete time tracking control becomes smaller than that under perfect tracking control. If parameter adaptation algorithm is combined with robust discrete time tracking control in order to estimate the uncertain parameter, the steady state performance is expected to be improved when the degree of parameter uncertainty is large. We are now preparing it and the result will appear in a near future.

## Appendix

A Derivation of (4), (5), (21), and (22)

$$\begin{aligned}
 \eta_1(k) &= A(z^{-1})\eta(k) & (A.1) \\
 |\eta_1(k)| &= |A(z^{-1})\eta(k)| \\
 &= |(1 + a_1z^{-1} + \dots + a_nz^{-n})\eta(k)| \\
 &\leq |\eta(k)| + |a_1\eta(k-1)| \\
 &\quad + \dots + |a_n\eta(k-n)| \\
 &\leq \mu m(k) + |a_1| \mu m(k-1) \\
 &\quad + \dots + |a_n| \mu m(k-n) \\
 &\leq \mu m(k) + |a_1| \mu \sigma^{-1} m(k) \\
 &\quad + \dots + |a_n| \mu \sigma^{-n} m(k)
 \end{aligned}$$

$$\leq \mu m(k) + \mu \sigma^{-n} m(k) \sum_{i=1}^n |a_i| \quad (\text{A.2})$$

$$\sum_{i=1}^n |a_i| \leq n \rho_1 \quad (\text{A.3})$$

so

$$\begin{aligned} |\eta_1(k)| &\leq \mu m(k) + \mu \sigma^{-n} m(k) n \rho_1 \\ &= \mu (1 + \sigma^{-n} n \rho_1) m(k) \\ &= \nu_1 \mu m(k) \end{aligned} \quad (\text{A.4})$$

where

$$\nu_1 = 1 + \sigma^{-n} n \rho_1.$$

Derivation of (21) and (22) follows the same procedure as above.

$$\eta_2(k) = A(z^{-1}) S_1(z^{-1}) \eta(k) \quad (\text{A.5})$$

$$\begin{aligned} |\eta_2(k)| &= |A(z^{-1}) S_1(z^{-1}) \eta(k)| \\ &= \left| \left(1 + \sum_{i=1}^n a_i z^{-i}\right) \left(1 + \sum_{i=1}^{d-1} s_i z^{-i}\right) \eta(k) \right| \\ &\leq |\eta(k)| + \left| \sum_{i=1}^{d-1} s_i \eta(k-i) \right| \\ &\quad + \left| \sum_{i=1}^n a_i \eta(k-i) \right| \\ &\quad + \left| \sum_{i=1}^n a_i z^{-i} \sum_{i=1}^{d-1} s_i z^{-i} \eta(k) \right|. \end{aligned} \quad (\text{A.6})$$

The first term of (A.6) becomes

$$|\eta(k)| \leq \mu m(k). \quad (\text{A.7})$$

The second term of (A.6) becomes

$$\begin{aligned} &\left| \sum_{i=1}^{d-1} s_i \eta(k-i) \right| \\ &\leq |s_1 \eta(k-1)| + |s_2 \eta(k-2)| + \dots + |s_{d-1} \eta(k-d+1)| \\ &\leq |s_1| \mu m(k-1) + |s_2| \mu m(k-2) + \dots + |s_{d-1}| \mu m(k-d+1) \\ &\leq |s_1| \mu \sigma^{-1} m(k) + |s_2| \mu \sigma^2 m(k) + \dots + |s_{d-1}| \mu \sigma^{-(d-1)} m(k) \\ &\leq \mu \sigma^{-(d-1)} m(k) \sum_{i=1}^{d-1} |s_i| \\ &\leq \mu \sigma^{-(d-1)} m(k) (d-1) \rho_2. \end{aligned} \quad (\text{A.8})$$

Similarly the third term of (A.6) becomes

$$\left| \sum_{i=1}^n a_i \eta(k-i) \right| \leq \mu \sigma^{-n} n \rho_1 m(k). \quad (\text{A.9})$$

The fourth term of (A.6) becomes

$$\begin{aligned} &\left| \sum_{i=1}^n a_i z^{-i} \sum_{i=1}^{d-1} s_i z^{-i} \eta(k) \right| \\ &= \left| (s_1 z^{-1} + s_2 z^{-2} + \dots + s_{d-1} z^{-(d-1)}) \sum_{i=1}^n a_i z^{-i} \eta(k) \right| \\ &\leq |s_1| \sum_{i=1}^n |a_i z^{-i-1} \eta(k)| + |s_2| \sum_{i=1}^n |a_i z^{-i-2} \eta(k)| + \dots + |s_{d-1}| \sum_{i=1}^n |a_i z^{-i-(d-1)} \eta(k)|. \end{aligned} \quad (\text{A.10})$$

Each term of the right hand side of last inequality (A.10) can be expressed as follows.

$$\begin{aligned} &\left| s_1 \sum_{i=1}^n a_i z^{-i-1} \eta(k) \right| = \left| s_1 \sum_{i=1}^n a_i \eta(k-i-1) \right| \\ &\leq |s_1| [ |a_1 \eta(k-2)| + |a_2 \eta(k-3)| + \dots + |a_n \eta(k-n-1)| ] \\ &\leq |s_1| [ |a_1| \mu m(k-2) + |a_2| \mu m(k-3) + \dots + |a_n| \mu m(k-n-1) ] \\ &\leq |s_1| \mu [ |a_1| \sigma^{-2} m(k) + |a_2| \sigma^{-3} m(k) + \dots + |a_n| \sigma^{-n-1} m(k) ] \\ &\leq |s_1| \mu \sigma^{-n-1} m(k) \sum_{i=1}^n |a_i| \\ &\leq |s_1| \mu \sigma^{-n-(d-1)} m(k) \sum_{i=1}^n |a_i| \end{aligned} \quad (\text{A.11})$$

$$\begin{aligned} &\left| s_2 \sum_{i=1}^n a_i z^{-i-2} \eta(k) \right| \\ &\leq |s_2| \mu \sigma^{-n-2} m(k) \sum_{i=1}^n |a_i| \\ &\leq |s_2| \mu \sigma^{-n-(d-15)} m(k) \sum_{i=1}^n |a_i| \end{aligned} \quad (\text{A.12})$$

$$\begin{aligned} &\vdots \\ &\left| s_{d-1} \sum_{i=1}^n a_i z^{-i-(d-1)} \eta(k) \right| \\ &\leq |s_{d-1}| \mu \sigma^{-n-(d-1)} m(k) \sum_{i=1}^n |a_i|. \end{aligned} \quad (\text{A.13})$$

Substituting (A.11), (A.12), and (A.13) into (A.10) leads to

$$\begin{aligned} &\left| \sum_{i=1}^n a_i z^{-i} \sum_{i=1}^{d-1} s_i z^{-i} \eta(k) \right| \\ &\leq (|s_1| + |s_2| + \dots + |s_{d-1}|) \\ &\quad \cdot \mu \sigma^{-n-(d-1)} m(k) \sum_{i=1}^n |a_i| \\ &\leq \rho_2 (d-1) \mu \sigma^{-n-(d-1)} m(k) \rho_1 n \\ &= \rho_1 \rho_2 n (d-1) \mu \sigma^{-n-(d-1)} m(k). \end{aligned} \quad (\text{A.14})$$

Substituting (A.7), (A.8), (A.9) and (A.14) into (A.6) leads to

$$\begin{aligned} |\eta_2(k)| &\leq [ 1 + \rho_2 (d-1) \sigma^{-(d-1)} + \rho_1 n \sigma^{-n} \\ &\quad + \rho_1 \rho_2 n (d-1) \sigma^{-n-(d-1)} ] \mu m(k) \\ &\leq [ 1 + 3 \rho_1 \rho_2 n (d-1) \sigma^{-n-(d-1)} ] \mu m(k). \end{aligned} \quad (\text{A.15})$$

## References

Anderson, B. D. O. and Moore, J. B., 1971, *Linear Optimal Control*, Prentice Hall, Englewood Cliffs, N. J.

Higuchi, T., Mizuno, T., Sugai, H. and Yun, C., 1984, "Primary Study on Applications of Electro-Hydraulic Servo Mechanism to Noncircular Cutting by a Lathe," *SEISAN-KENKYU*, Institute of Industrial Science, University of Tokyo, Vol. 36, No. 2, pp. 71~73.

Kreisselmeier, G. and Anderson, B. D. O., 1986, "Robust Model Reference Adaptive Control," *IEEE Trans. Automatic Control*, Vol. AC-31, No. 2, pp. 127~133.

Landau, I. D. and Lozano, R., 1981, "Unification and Evaluation of Discrete Time Explicit Model Reference Adaptive Design," *Automatica*, Vol. 17, No. 4, pp. 593~611.

Sarpturk, S.Z., Istefanopulos, Y. and Kaynak, O., 1987, "On the Stability of Discrete-Time

Sliding Mode Control Systems," *IEEE Trans. Automatic Control*, Vol. AC-32, No. 10, pp. 930~932.

Tomizuka, M. and Whitney, D. E., 1975, "Optimal Discrete Finite Preview Problem(Why and How is Future Information Important?)," *ASME Journal of Dynamic Systems, Measurement and Control*, Vol. 97, No. 4, pp. 319~325.

Tomizuka, M. et al., 1987, "Tool Positioning for Noncircular Cutting with Lathe," *ASME Journal of Dynamic Systems, Measurement and Control*, Vol. 109, No. 2, pp. 176~179.

Utkin, V. I., 1977, "Variable Structure Systems with Sliding Modes," *IEEE Trans. Automatic Control*, Vol. AC-22, No. 2, pp. 212~222.